Eur Biophys J (2012) 41:615–627
DOI 10.1007/s00249-012-0829-1

ORIGINAL PAPER

EBSA
Biophysics in Europe

Resolution of the effects induced by W → F substitutions on the conformation and dynamics of the amyloid-forming apomyoglobin mutant W7FW14F

Giuseppe Infusini · Clara Iannuzzi · Silvia Vilasi · Leila Birolo · Daniela Pagnozzi · Piero Pucci · Gaetano Irace · Ivana Sirangelo

Received: 20 March 2012 / Accepted: 28 May 2012 / Published online: 22 June 2012
© European Biophysical Societies' Association 2012

Abstract Myoglobin is an alpha-helical globular protein containing two highly conserved tryptophanyl residues at positions 7 and 14 in the N-terminal region. The simultaneous substitution of the two residues increases the susceptibility of the polypeptide chain to misfold, causing amyloid aggregation under physiological condition, i.e., neutral pH and room temperature. The role played by tryptophanyl residues in driving the folding process has been investigated by examining three mutated apomyoglobins, i.e., W7F, W14F, and the amyloid-forming mutant W7FW14F, by an integrated approach based on far-ultraviolet (UV) circular dichroism (CD) analysis, fluorescence spectroscopy, and complementary proteolysis. Particular attention has been devoted to examine the conformational and dynamic properties of the equilibrium intermediate formed at pH 4.0, since it represents the early organized structure from which the native fold originates. The results show that the W → F substitutions at position 7 and 14 differently affect the structural organization of the AGH subdomain of apomyoglobin. The combined effect of the two substitutions in the double mutant impairs the formation of native-like contacts and favors interchain interactions, leading to protein aggregation and amyloid formation.

Keywords Apomyoglobin · Protein folding · Protein misfolding · Amyloid aggregation

Introduction

Proteins spontaneously fold from randomly unfolded conformations to biologically active structures in a hierarchical manner, with secondary structure preceding tertiary structure formation (Baldwin and Rose 1999). Secondary structure is primarily stabilized by hydrogen bonds between the amide groups of amino acids that are close in sequence (Aurora et al. 1997; Baldwin 2003), whereas tertiary structure is stabilized by hydrophobic interactions among side-chains of more distant segments of the chain (Kauzmann 1959; Tanford 1973). This is supported by the observation that fluctuating elements of secondary structure often persist under denaturing conditions where the chain is disordered and devoid of specific tertiary interactions. Under physiological conditions, hydrophobic interactions among nonpolar side-chains favor collapse of hydrogen-bonded secondary structure elements into a compact conformation (Dill 1985). In this respect, folding is usually envisaged as the convergence of an ensemble of disordered conformations, i.e., the unfolded

Giuseppe Infusini, Clara Iannuzzi, and Silvia Vilasi contributed equally to this work.

G. Infusini · L. Birolo · D. Pagnozzi · P. Pucci
Dipartimento di Chimica Organica e Biochimica, Università di Napoli "Federico II", Complesso Monte S. Angelo, Naples, Italy

C. Iannuzzi · G. Irace · I. Sirangelo (✉)
Dipartimento di Biochimica e Biofisica, Seconda Università di Napoli, Via L. De Crecchio 7, 80138 Naples, Italy
e-mail: ivana.sirangelo@unina2.it

C. Iannuzzi
MRC-National Institute for Medical Research, London NW7 1AA, UK

S. Vilasi
CNR-Istituto di Biofisica, Via U. La Malfa 153, 90146 Palermo, Italy

G. Irace · I. Sirangelo
Istituto Nazionale Biostrutture e Biosistemi, Rome, Italy

state, toward lower-energy partially folded compact structures from which the biologically active protein is obtained (Kim and Baldwin 1990).

Apomyoglobin, i.e., heme-free myoglobin, is a small, alpha-helical protein that contains two highly conserved tryptophanyl residues located at positions 7 and 14 in the N-terminal region of the molecule (Fig. 1). The folding of this protein is known to proceed through compact intermediates that have been detected in both kinetic and equilibrium experiments (Hughson et al. 1990; Kay and Baldwin 1996; Barrick and Baldwin 1993; Sirangelo et al. 1998, 2003a, b). In most of these intermediates, A, G, and H helices are folded and sterically oriented as in the native AGH subdomain, whereas the remainder of the molecule seems to be unordered. More recently, Uzawa et al. (2004) presented evidence that the high level of helical structure in the earliest compact intermediate suggests the presence of helical regions outside the A, G, and H helix subdomain. Furthermore, the same authors supposed that the increases in helix content observed in the subsequent folding stages are probably due to an increase in the length of the pre-existing helices.

Our previous results indicated that the tryptophanyl residues are strong determinants of apomyoglobin structure and that the presence of at least one of the two residues is necessary for the formation of tertiary key interactions in the early stages of protein folding (Sirangelo et al. 2000). The simultaneous replacement of both tryptophanyl residues affects the folding pathway, causing aggregation and formation of amyloid-like fibrils at physiological pH (Sirangelo et al. 2002, 2004). On the contrary, wild-type apomyoglobin was reported to form amyloid fibrils only under stress conditions that favor the association of unfolded polypeptide segments (Fandrich et al. 2003; Vilasi et al. 2011).

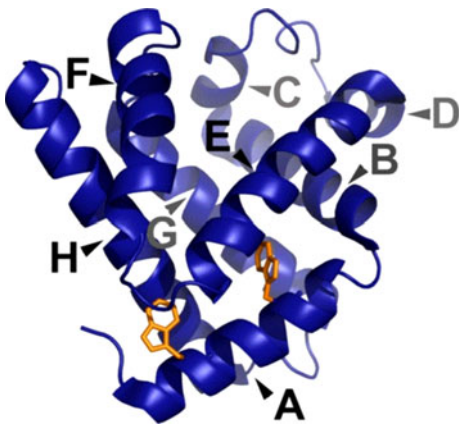

Fig. 1 X-ray structure of wild-type sperm whale apomyoglobin (PDB accession no. 2JHO). Helices are labeled from A to H, and the side-chains of the conserved tryptophans (positions 7 and 14) are shown in the structure

Protein aggregation is known to occur naturally in nonpathological states when proteins fail to fold properly (Kopito 2000; Ben-Zvi and Goloubinoff 2001) or when its folded structure converts into a conformational state that is at least partially unfolded and prone to aggregation (Kelly 1996; Rochet and Lansbury 2000). Natural mutations associated with familial forms of amyloidosis have been shown to reduce the stability of the folded state (Hurle et al. 1994; Quintas et al. 2001; Canet et al. 2002; Niraula et al. 2002). Recent studies have allowed three major factors to be identified as important parameters in the conversion of the partially or totally unfolded state of a protein into aggregates. These are high hydrophobicity, high propensity to convert from α-helical to β-sheet structure, and low net charge (Konno 2001; Chiti et al. 2002; Tjernberg et al. 2002; Ciani et al. 2002; Monsellier et al. 2007; Tartaglia et al. 2008). In the case of the W7FW14F apomyoglobin mutant, an increased hydrophobicity of the N-terminal segment and tendency to form β-strands has been reported (Jennings and Wright 1993; Sirangelo et al. 2004).

In this study, we used an integrated approach based on far-UV CD analysis, fluorescence spectroscopy, and complementary proteolysis to investigate the conformational effects produced by single-point W → F mutations introduced at position 7 and 14, in order to understand how their combination makes the polypeptide chain highly prone to form amyloid under physiological conditions. In addition, we performed prediction analysis that helped to elucidate the molecular events underlying the aggregation process. We focused most of our attention on the conformational and dynamic properties of the partially folded state formed at pH 4.0, since it represents the early organized structure from which the native protein fold originates (Jennings and Wright 1993; Eliezer et al. 1998; Tsui et al. 1999; Jamin 2005). The behavior of single W → F mutants at pH 4.0 was compared with that of the amyloid-forming double mutant at pH 4.0, where it is soluble without any tendency to aggregate. Moreover, detailed characterization of the native state of wild-type and single mutants was also carried out. This could not be done for the double mutant because of the aggregation occurring at neutral pH.

The results presented in this paper show that the W → F substitutions at position 7 and 14 differently affect the structural organization and the flexibility of the AGH subdomain of apomyoglobin. The combination of the two effects in the double mutant determines further changes that make the polypeptide chain more susceptible to aggregation and amyloid formation. Controlled proteolysis experiments were employed to analyze the final aggregation product of the double mutant, i.e., the amyloid-like fibrillar form. This contributed to elucidate the molecular events leading the protein to deviate from the productive folding process.

Experimental procedures

Protein expression and purification

Wild-type sperm whale myoglobin was obtained by expressing the synthetic gene in *Escherichia coli* strain TB-1 [ara, Δ (lac-pro), strA, thi, Φ80dlacZΔM, r−, m+] (Springer and Sligar 1987). The tryptophanyl substitutions were performed as described elsewhere (Sirangelo et al. 2000). Wild type, and W7F and W14F mutants were essentially purified as described by Springer and Sligar (1987). The culture was grown at 37 °C in Luria–Bertrani broth in the presence of ampicillin (200 mg/l), harvested in late log phase, lysed in lysis buffer [50 mM Tris-HCl, 1.0 mM ethylenediaminetetraacetic acid (EDTA), 0.5 mM dithiothreitol (DTT), 40 units of DNase per ml, 3 units of RNase A per ml, 4 mg of lysozyme per ml, pH 8.0] at 4 °C overnight, and sonicated for 30 min on ice. Cell debris was removed by centrifugation, and the supernatant was fractionated by ammonium sulfate precipitation. The 60–95 % cut was centrifuged and suspended in 20 mM Tris and 1.0 mM EDTA (pH 8.0) and fractionated on a Sephadex G-50 (Pharmacia) gel filtration column (2.5 × 100 cm) equilibrated in the same buffer. Fractions containing reddish-brown myoglobin were collected and applied to a Whatman DEAE 52 ion-exchange column (2.5 × 20 cm) equilibrated and resolved with 20 mM Tris-HCl (pH 8.4). Under this conditions the myoglobin did not stick on the column and was rapidly eluted. Protein purity was controlled by sodium dodecyl sulfate polyacrylamide gel electrophoresis (Laemmli 1970). The heme was removed from myoglobin by the 2-butanone extraction procedure (Teale 1959). The contamination of the apoprotein by myoglobin was assessed spectrophotometrically. In all cases, no significant absorption was observed in the Soret region. W7FW14F myoglobin mutant was purified as N-terminal His-tagged form via affinity chromatography on Ni^{2+}-nitrilotriacetic acid resin as previously described (Sirangelo et al. 2002, 2004). The His-tag was not removed, because it does not affect the double mutant properties. This was previously verified using the TAGZyme system (Quiagen) after subcloning in pQE1 (unpublished data) and by comparing with His-tagged wild-type protein (Sirangelo et al. 2002, 2004). Protein concentration was determined under denaturing conditions by measuring absorption at 280 nm for wild type, and W7F and W14F mutants and at 275 nm for W7FW14F mutant. The molar extinction coefficients, calculated from the tryptophan and tyrosine content (Wetlaufer 1962; Edelhoch 1967), were $\varepsilon_{280} =$ 13,500, and 9,750 M^{-1} cm^{-1} for wild-type and single-tryptophanyl-substituted myoglobins, respectively, and $\varepsilon_{275} =$ 3,750 M^{-1} cm^{-1} for W7FW14F mutant. The absorption measurements were carried out on a Jasco V-550 spectrophotometer.

Fluorescence

Fluorescence measurements were performed on a Perkin-Elmer LS 55 fluorescence spectrophotometer using emission and excitation bandwidths of 3.5 nm and cell with optical path length of 1 cm. To avoid contamination from tyrosine emission, protein samples were excited at 295 nm, a wavelength at which the absorption of this residue is negligible. The temperature was maintained at 25 °C. Fluorescence quenching experiments were performed by adding small aliquots of a 5.0 M acrylamide to an 8.0 μM protein solution. The fluorescence intensities were corrected for dilution caused by the stepwise addition of quencher. The values of the dynamic quenching constant (Stern–Volmer constant, K_{SV}) were obtained by fitting the experimental data to the equation

$$\frac{F_0}{F} = (1 + K_{SV}[Q]) \times e^{(K_{ST}[Q])},$$

where F_0 and F are the fluorescence intensities in the absence and presence of quencher, respectively, [Q] is the concentration of quencher, and K_{ST} represents the static quenching constant responsible for the appearance of an upward curvature of the plot (Eftink and Ghiron 1976).

CD spectroscopy

The far-UV CD spectra were recorded at 25 °C on a Jasco J-715 spectropolarimeter at protein concentration of 20 μM using thermostated quartz cells of 0.1 cm path length. Spectral acquisition was taken at 0.2 nm intervals with 4 s integration time and bandwidth of 1.0 nm. An average of three scans was obtained for all of the spectra. Photomultiplier absorbance did not exceed 600 V in the spectral region analyzed. Data were corrected for buffer contributions and smoothed using the software provided by the manufacturer (System Software version 1.00). All measurements were performed under nitrogen flow. The results are expressed as mean residue ellipticity $[\Theta]_{MRW}$ in units of degrees cm^2 $dmol^{-1}$. A mean residue weight of 115 was used for the peptide chromophore. Protein secondary structure estimation was performed using CDPro software, which contains three software packages, i.e., CDSSTR, CONTIN/LL, and SELCON3 (Sreerama and Woody 2000). The secondary structure percent contents reported are the arithmetic means of the estimates obtained from each program.

Complementary proteolysis experiments

Enzymatic hydrolysis were performed at 37 °C by incubating the sample in 10 mM Tris–HCl, pH 7.0 for the experiments at pH 7.0, or ammonium acetate 10 mM, pH 4.0 for the experiments at pH 4.0 with enzyme-to-substrate ratios ranging from 1:1,000 to 1:50 (w/w). Trypsin, chymotrypsin, endoprotease K, and endoprotease Glu-C were

used as conformational probes at pH 7.0, whereas endoprotease V8 and pepsin were selected for digestion at pH 4.0 due to their activity at acidic pH. The extent of proteolysis was monitored on a time-course basis by sampling the reaction mixture at different time intervals from 15 to 60 min. Digested protein samples were acidified to pH 2.5 by adding trifluoroacetic acid (TFA), and proteolytic fragments were separated by reverse-phase high-performance liquid chromatography (HPLC) on a Phenomenex Jupiter C18 column (250 × 2.1 mm, 300 Å pore size) with a linear gradient of 5–65 % acetonitrile in 0.1 % TFA over 60 min, at flow rate of 200 µl/min. Elution was monitored at 220 and 280 nm. Individual fractions were collected and analyzed by electrospray mass spectrometry using a ZQ instrument. Data were acquired and processed using MassLynx software purchased by the manufacturer.

Limited proteolysis on W7FW14F apomyoglobin fibrils

For enzymatic digestion, fibrils were separated by centrifugation (13,000 rpm, 10 min), resuspended with the original buffer, and collected again by centrifugation. This procedure was repeated three times. The samples were finally resuspended with 200 µl 10 mM sodium phosphate, pH 7.0, and the absence of any residual soluble form checked by matrix-assisted laser desorption/ionization time-of-flight (MALDI-TOF) analysis. Proteases (1 µg/ml trypsin, 0.5 µg/ml chymotrypsin, 1:100, 1 µg/ml elastase, 0.2 1 µg/ml Glu-C, respectively, in 10 mM sodium phosphate buffer, pH 7.0) were added, and digestion allowed to proceed for 15 min at 37 °C. After 15 min, the digested fibrils were collected by centrifugation and the reaction was then stopped by acidification with TFA 0.1 % final concentration. One microliter was mixed with 1 µl of a solution of α-cyano-4-hydroxycinammic acid, 10 mg/ml in 70 % acetonitrile, 30 % 50 mM citric acid, and the mixture was applied onto the metallic sample plate, air-dried, and analyzed by MALDI time-of-flight mass spectrometry using a Voyager STR mass spectrometer (Applied Biosystems). Mass calibration was performed using a peptide standard mixture provided by the manufacturer. All mass values are reported as monoisotopic masses, and raw data were analyzed using software provided by the manufacturer.

Calculation of aggregation propensities

Prediction analyses were performed using online available predictors such as TANGO, PASTA, and CamP. The apoMb amino acid sequences were analyzed for β-aggregation propensity using Tango (Fernandez-Escamilla et al. 2004), PASTA (Trovato et al. 2007), and Zyggregator (Tartaglia et al. 2008), and for tendency of proteins to convert from the native state to the amyloid state using Zagg + CamP (Tartaglia et al. 2007).

Results

Circular dichroism

The effects caused by W → F substitutions on the structure of the native and partially unfolded state of apomyoglobin were investigated by circular dichroism and fluorescence. Figure 2a shows the CD spectra recorded at neutral pH and 25 °C for soluble native apomyoglobins, i.e., wild type and single mutants W7F and W14F. All spectra exhibit two negative minima at 222 and 208 nm, typical of polypeptide chains mostly in α-helical conformation. The estimated secondary structure compositions are displayed in Table 1. The results indicate that the α-helical content of single-tryptophan-containing apomyoglobins is slightly lower than that of wild-type protein, thus suggesting that each single-tryptophanyl substitution at either position 7 or 14 affects protein secondary structure. Unfortunately, the CD spectra of the native folded single-substituted apomyoglobins at neutral pH could not be directly compared with that of W7FW14F because of the aggregation occurring at this pH value, which brings the protein into a nonnative

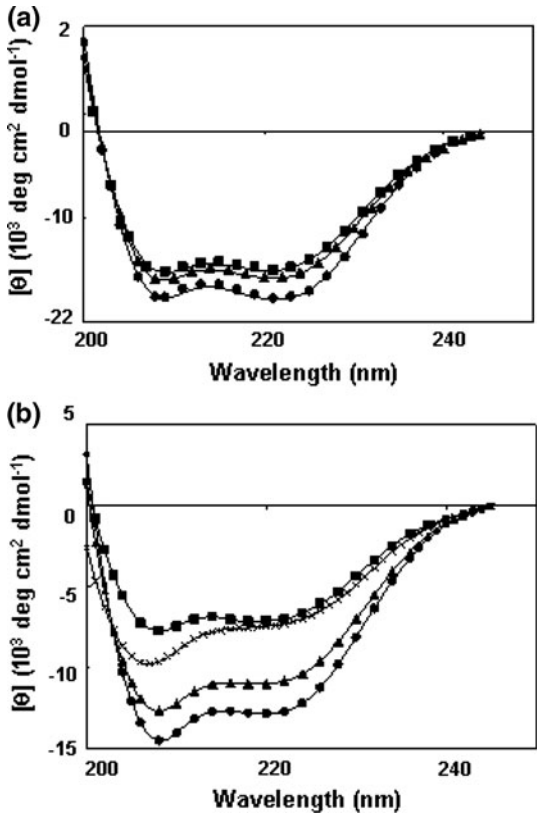

Fig. 2 Far-UV circular dichroism spectra of wild-type (*filled circles*), W7F (*filled squares*), and W14F (*filled triangles*) apomyoglobins at pH 7.0 (**a**) and pH 4.0 (**b**), and W7FW14F apomyoglobin (*crosses*) at pH 4.0 (**b**). Spectra were recorded at 25 °C in 10 mM phosphate/acetate buffer at protein concentration of 20 µM

Table 1 Percent content of secondary structure of wild-type and mutant apomyoglobin at neutral and acidic pH

pH 7.0	wt	W7F	W14F	W7FW14F[a]
α	0.65	0.52	0.56	0.56
β	0.04	0.09	0.07	0.09
Turn	0.09	0.14	0.12	0.14
Unordered	0.22	0.25	0.25	0.021
pH 4.0	wt	W7F	W14F	W7FW14F
α	0.46	0.26	0.37	0.28
β	0.10	0.23	0.13	0.22
Turn	0.17	0.21	0.21	0.22
Unordered	0.27	0.30	0.29	0.28

[a] Data from Iannuzzi et al. (2007). Analysis was performed on computed CD spectrum extrapolated from the time dependence of dichroic activity

amyloid conformation (Sirangelo et al. 2004). Nevertheless, the CD spectrum of the amyloidogenic apomyoglobin could be extrapolated from the time dependence of the CD activity (Iannuzzi et al. 2007), and the estimated secondary structure is presented in Table 1 and compared with that of wild-type and single-substituted apomyoglobins.

At pH 4.0, the negative ellipticity of wild-type and single-tryptophan-substituted apomyoglobins decreases, but the spectra still exhibit the two characteristic minima (Fig. 2b). However, the substitution W → F at position 7 seems to affect the secondary structure composition to a larger extent, causing an increase in the content of β-structure and a decrease of helical content (Table 1). The secondary structure content of the amyloid-forming W7FW14F apomyoglobin mutant at pH 4.0, i.e., in conditions for which the polypeptide is in a soluble partially folded conformation (Sirangelo et al. 2002, 2004), is very similar to that of W7F.

Complementary proteolysis experiments

Complementary proteolysis experiments were carried out on the equilibrium intermediate formed at pH 4.0 of W7FW14F in comparison with wild type, W14F, and W7F. Due to their activity at acidic pH, endoprotease V8, which specifically cleaves at the C-terminal glutamic acid, and pepsin, which is a rather nonspecific enzyme, were selected for digestion, with the aim of creating conditions in which the selectivity of the cleavage was not related to, or limited by, the specificity of the enzyme. An appropriate enzyme-to-substrate ratio was selected in each case to achieve single proteolytic events on the intact molecule. Under these conditions, the protein remained largely undigested, with only a limited number of fragments released from the molecule. The extent of the enzymatic hydrolysis was monitored on a time-course basis by sampling the incubation mixture at different time intervals followed by HPLC fractionation. The fragments generated from the protein were identified by their unique mass values as obtained by electrospray mass spectrometry (ESMS) leading to the assignment of cleavage sites. Only the first cleavage event in each molecule was considered as reflecting structural information, since the original structure of the protein can be altered after the first cleavage.

An example HPLC chromatogram of the sample of W7FW14F withdrawn after 15 min of incubation with endoprotease V8 at pH 4.0 (E/S ratio 1/600 w/w) is shown in Fig. 3.

W7FW14F was cleaved at Glu136, releasing the complementary fragments 1–136 and 137–153 (peaks 4 and 1 in Fig. 3, respectively). Moreover, peak 2 and peak 3 were identified as peptides 39–153 and 86–153, whose complementary peptides were found in fraction 4 (peptide 1–85)

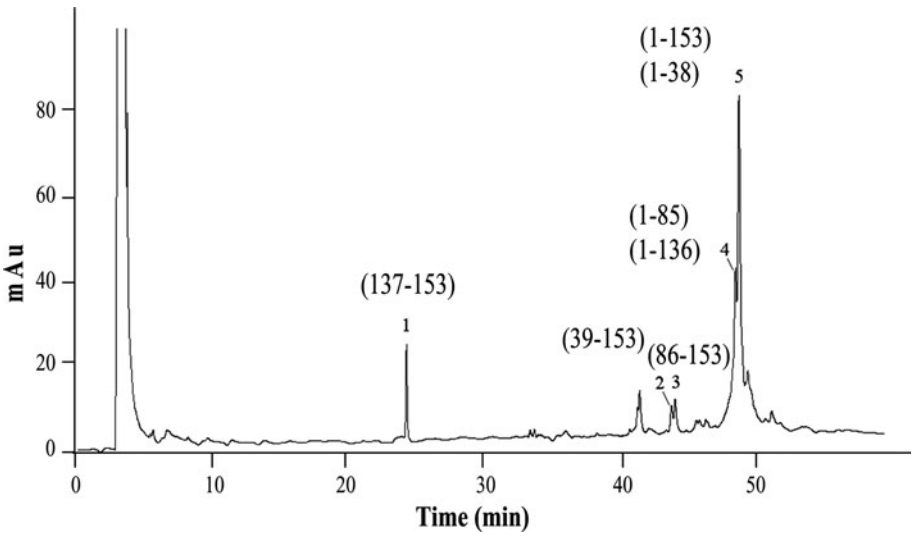

Fig. 3 Complementary proteolysis experiments. HPLC profile of the aliquot withdrawn after 15 min incubation of W7FW14F with endoprotease V8 at pH 4.0 under controlled conditions using E/S ratio of 1/600 (w/w). Individual fractions were collected and identified by ESMS, and the corresponding peptides are reported

and fraction 5 (peptide 1–38), indicating the occurrence of cleavage sites at Glu38 and Glu85.

The cleavage sites identified in the limited proteolysis experiments on W7FW14F in comparison with wild type, W14F, and W7F are shown in Fig. 4b. In W7FW14F, preferential proteolytic sites were identified at Leu29, Glu38, Glu85, Glu109, and Glu136. Leu29, Glu38, Glu85, and Glu136 were also cleavage sites in wild-type apomyoglobin as well as in the single mutants, whereas cleavage at Glu109 was observed only in W7F besides the double mutant. Additional cleavage sites at Glu 54 and Leu69 were observed in all the proteins except in W7FW14F, whereas cleavage at Glu105 was specifically detected only in W7F.

The overall analysis of the proteolytic patterns reveals few but significant differences between W7FW14F and wild-type protein, since in the double mutant the region corresponding to helices D and E in the native fold are protected from proteases, while helix G is exposed, thus suggesting significant differences in the structural organization. The pattern of cleavage sites of W14F is identical to wild type, with all the helices, except A and G, accessible to proteases, whereas in W7F also helix G is accessible.

Complementary proteolysis experiments were carried out also at pH 7.0 on wild-type apomyoglobin and the single-tryptophan-containing mutants using trypsin, chymotrypsin, endoprotease K, and endoprotease Glu-C as conformational probes. The overall patterns of proteolytic sites exhibited by the three protein species in their native state are summarized in Fig. 4a. The proteolytic pattern of wild type was identical to that reported in literature (Fontana et al. 1997; Kim et al. 2005). In the case of the examined mutants, only W7F showed a further specific proteolytic cleavage at Glu136. As a whole, these results indicated that all apomyoglobins are compact with few specific regions amenable to protease action essentially located in the F helix. It should be underlined that this helix is involved in the interaction with heme in native myoglobin and is frayed upon removal of the prosthetic group (Eliezer and Wright 1996). However, the W7F mutant

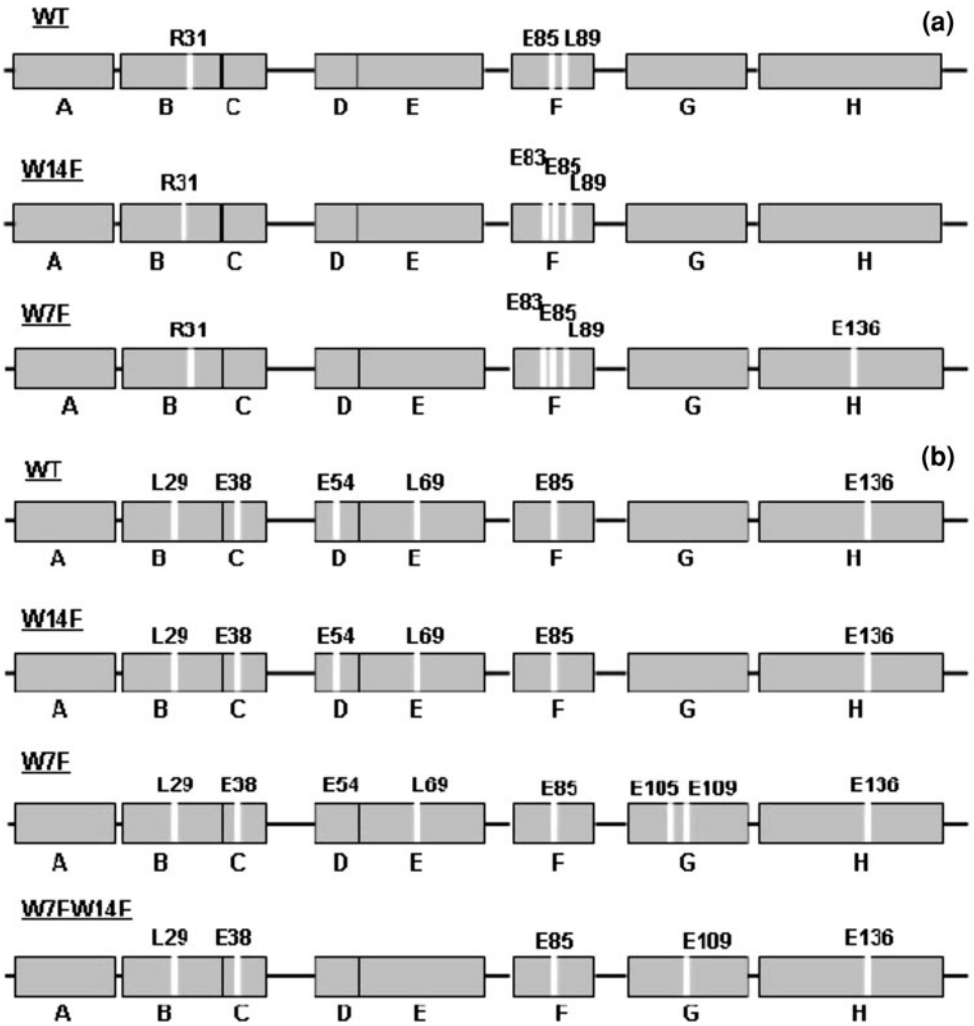

Fig. 4 Preferential cleavage site pattern observed in W7FW14F, wild-type, W7F, and W14F apomyoglobins at pH 7.0 (**a**) and 4.0 (**b**)

showed a peculiar accessibility within the H helix that was not observed in the other species. This result corroborates the CD analysis revealing a decrease of α-helix content in W7F apoMb which may be ascribed to a less structured H helix.

Fluorescence

The stability of the tryptophanyl microenvironment in the partially unfolded state at pH 4.0 was probed following the guanidine dependence of the intrinsic tryptophanyl fluorescence. Figure 5 shows the results plotted as the ratio between the intensities at 320 and 360 nm (F_{320}/F_{360}). This ratio is readily altered by changes in the solvent accessibility to indole residues, since the emission of solvent-exposed indole residues is considerably red-shifted compared with that of buried residues, i.e., 350–360 versus 320–330 nm (Irace et al. 1981). The three curves are superimposed, thus indicating that the stability of the tryptophanyl microenvironment in the equilibrium intermediate is not influenced by the introduced amino acid replacement at either position 7 or 14. These results are consistent with those reported by Dyuysekina et al. (2008), who studied the stability of apomyoglobin substituted at conserved W14. Moreover, the sigmoidal dependence of fluorescence emission on denaturant concentration reveals the cooperative destruction of tertiary interactions stabilizing the AGH subdomain.

In conclusion, the data so far reported indicate that single W → F substitution causes a decrease of helical content and stability (Sirangelo et al. 2000) of apomyoglobin in its native state but does not affect the stability of the tryptophanyl environments at pH 4.0 despite the difference observed in the secondary structure contents. This lets us hypothesize that the single substitutions determine a different structural organization of the molecular region clustering the indole residues without affecting the overall stability.

Fluorescence quenching

We used fluorescence quenching to evaluate the effects induced by single-point mutations on the local conformation and dynamics of tryptophanyl microenvironments. Previous studies indicated that the contribution to the total protein emission of the two tryptophans is rather additive, thus suggesting that they emit independently (Sirangelo et al. 2003a, b). Figure 6 shows the effect of increasing concentration of a neutral quencher, i.e., acrylamide, on the fluorescence intensity of the single-tryptophan-containing apomyoglobin mutants W7F and W14F at acidic pH in comparison with the wild-type protein. The data were analyzed in terms of the Stern–Volmer equation, plotting the dependence of the fluorescence ratio F_0/F measured at 320 nm (F_0 denotes the fluorescence intensity in the absence of quencher) versus quencher concentration. Table 2 presents the Stern–Volmer constants calculated from the data reported in Fig. 6, compared with those obtained at pH 7.0 previously reported (Sirangelo et al. 2003a, b). The increased values detected for the single-substituted apomyoglobins at both pH values indicate that the replacement of one tryptophanyl residue increases the solvent accessibility of the other. Moreover, the Stern–Volmer constants relative to the acrylamide quenching of wild-type protein is almost unchanged at pH 4.0 with respect to pH 7.0, whereas those of the two single-tryptophan-containing apomyoglobin are slightly higher. This indicates that the introduced amino acid replacement alters

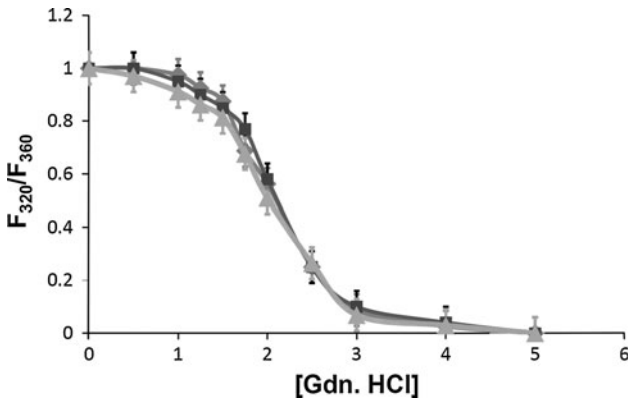

Fig. 5 Dependence of tryptophanyl fluorescence intensity ratio at 320 and 360 nm on guanidine concentration of wild-type (*filled diamonds*), W7F (*filled squares*), and W14F (*filled triangles*) apomyoglobins at pH 4.0. Data are expressed as percent variation. Excitation was at 295 nm. Protein concentration was 8 μM in 10 mM phosphate/acetate buffer

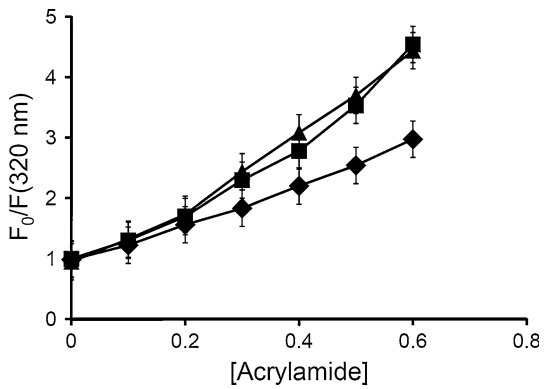

Fig. 6 Acrylamide quenching of wild-type (*filled diamonds*), W7F (*filled squares*), and W14F (*filled triangles*) apomyoglobins at pH 4.0. *Solid lines* were obtained by fitting the experimental data to the equation $F_0/F = (1 + K_{SV}[Q]) \times \exp(K_{ST}[Q])$. The excitation wavelength was 295 nm. Protein concentration was 8 μM in 10 mM phosphate/acetate buffer. Temperature was kept at 25 °C

Table 2 Stern–Volmer constant (K_{SV}) for acrylamide quenching of wild-type and mutant apomyoglobins at neutral and acidic pH

	pH 4.0	pH 7.0[a]
Wild type	3.5	3.2
W7F	6.0	5.1
W14F	5.9	5.0

[a] Data from Sirangelo et al. (2003a, b)

the structure and dynamics of the AGH subdomain in the equilibrium intermediate more than in the native state.

Characterization of the amyloid-like fibrils and prediction analysis

The amyloid product formed at pH 7.0 by W7FW14F was analyzed using controlled proteolysis experiments in conjunction with MALDI-MS analysis of the fragments generated. This investigation aimed to describe the protein regions involved in the stable core of the fibrils. The rationale behind this approach is that proteolytic cleavages on the fibrils would only occur at flexible regions of the polypeptide chain, leaving the inaccessible core untouched (Monti et al. 2005).

Fibrils were washed accurately before enzyme incubation to remove any possible soluble component, thus avoiding misleading results. After centrifugation, the recovered pellet was diluted in the working buffer and individually incubated with trypsin, chymotrypsin, Glu-C, and elastase as proteolytic enzymes. At appropriate digestion times, aliquots of the samples were centrifuged and the supernatant analyzed by MALDI-MS. Fibril-released fragments were identified on the basis of the mass value and the protease specificity. Table 3 presents the results obtained with the four proteases.

The distribution of cleavage sites observed in the fibrils from W7FW14F is summarized in Fig. 7. Proteolytic experiments revealed a picture of the fibril structure in which helices A, B, and E and part of helices D and G are protected from protease action and, thus, are possibly involved in the fibril core.

Moreover, we used some of the online available predictors, such as TANGO, PASTA, and Zyaggregator, to evaluate whether changes in the properties of the sequence are sufficient to explain our observations or, instead, structural modifications of the amyloidogenic double mutant need to be invoked. Tango revealed the presence of β-aggregating sequences in wild-type protein corresponding to segments 6–15, 66–75, and 101–108, which belong to helices A, E, and G, respectively, in the natively folded protein (Fig. 8). Both single substitutions W7F and W14F slightly increase the β-aggregation propensity of segment 6–15, but their simultaneous occurrence has a much larger effect, determining a four time increase. Regions 6–15 and 101–108 were also predicted by PASTA to have β-aggregation tendencies, albeit the latter at a comparatively higher level (Fig. 9). Interestingly, PASTA revealed that the W → F replacement at position 7 does not affect the aggregating propensity of segment 6–11, whereas it increases almost twofold for the other substitution. The same three regions were predicted by Zyggregator but without significant differences among mutants. The most relevant aspect of the prediction analysis is that the β-aggregating sequences correspond to the protein regions that are fully protected from protease action on mature fibrils and, thus, are possibly involved in the formation of the fibril core. Significant differences were observed using Zagg + CamP, which predicts the

Table 3 MALDI-TOF analysis of protease-digested W7FW14F apomyoglobin fibrils

Protease	Identified peptide	Experimental [MH^+] mass value (Da)	Theoretical [MH^+] mass value (Da)
GLU-C	39–54	1,992.04	1,992.05
	39–52	1,791.81	1,791.97
	42–54	1,648.74	1,648.88
	42–52	1,448.68	1,448.79
	110–136	2,854.46	2,854.45
	137–148	1,481.72	1,481.85
	137–153	2,000.94	2,001.11
Trypsin	32–47	2,022.41	2,022.08
	32–45	1,747.13	1,746.9
	35–47	1,634.08	1,633.83
	35–45	1,358.87	1,358.67
	79–96	1,982.38	1,982.05
	80–96	1,853.92	1,853.96
	140–147	936.88	936.56
Chymotrypsin	15–29	1,523.83	1,522.78
	34–46	1,633.84	1,633.83
	34–43	1,215.63	1,215.63
	116–123	951.45	951.45
	139–153	1,739.96	1,739.96
Elastase	40–53	1,761.78	1,761.96
	78–94	1,880.95	1,881.0
	108–123	1,813.85	1,813.95
	131–144	1,619.88	1,619.90

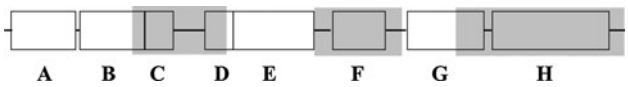

Fig. 7 Regions protected from protease action in W7FW14F fibrils. *Highlighted in grey* are the regions corresponding to peptides found in the supernatant of W7FW14F fibril digestions with proteases

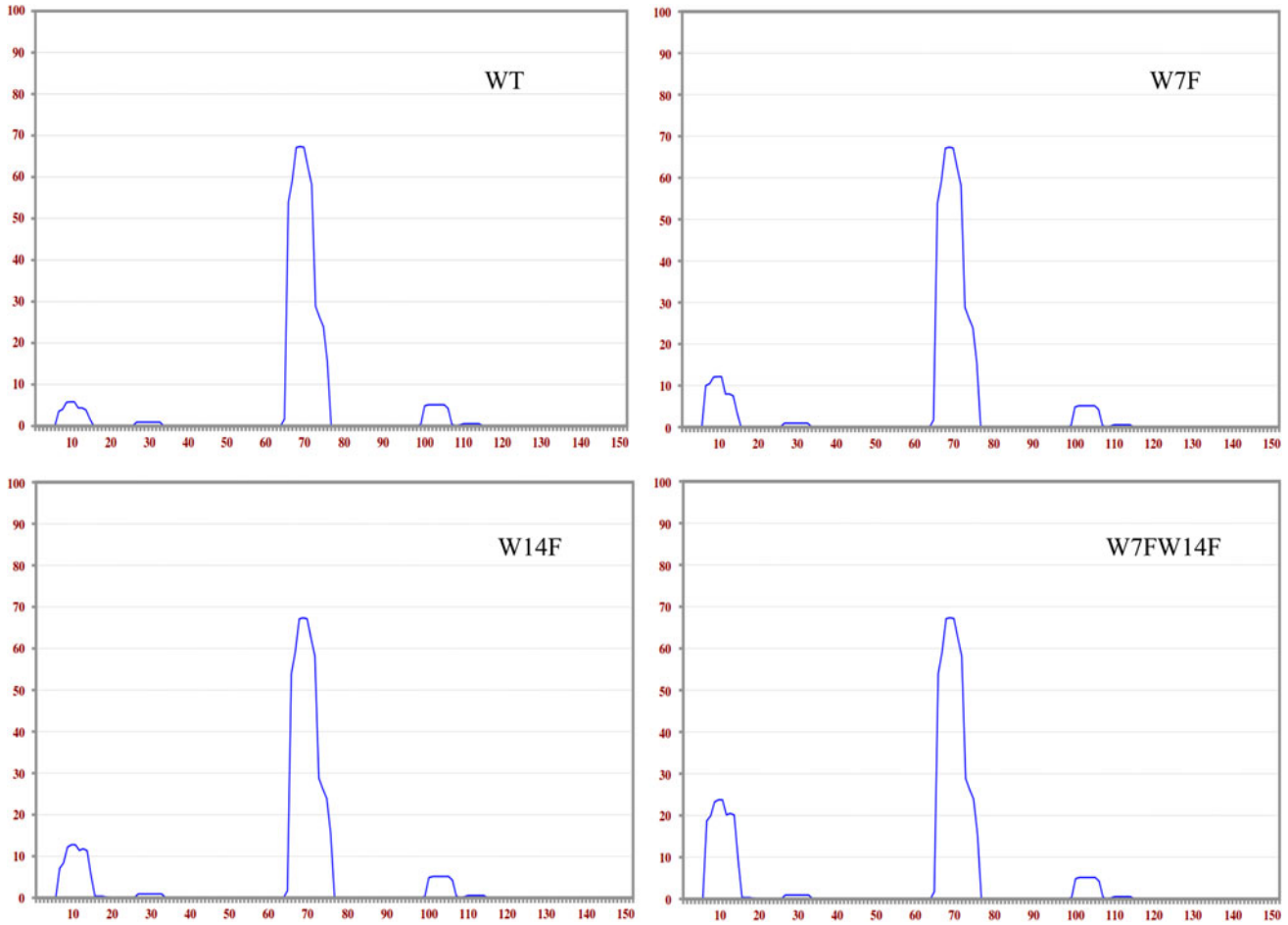

Fig. 8 Prediction of apomyoglobin β-aggregation propensity based on TANGO aggregation scores of wild type and W7F, W14F, and W7FW14F mutants

tendency of proteins to convert from the native state to the amyloid state. The results are shown in Fig. 10. Their analysis reveals that the W → F replacement at position 7 increases the propensity of the protein to undergo local unfolding events which may trigger the $\alpha \rightarrow \beta$ transition responsible for β-aggregation.

Discussion

The ability to form amyloid fibrils is a generic property of polypeptide chains and can be readily rationalized (Dobson 1999, 2002). The amyloid core structure results primarily from the formation of a network of hydrogen bonds involving the amide and carbonyl groups of the polypeptide backbone that links the β-strands together. In essence, in amyloid fibrils the main chain dominates the structure and the side-chains are incorporated in the most favorable manner consistent with this requirement. By contrast, in the evolved globular structures, the overall fold is determined by the close-packing of the side-chains, and the polypeptide backbone is incorporated in the most favorable manner. Globular proteins may then have evolved features to prevent aggregation by selecting and preserving key residues that interfere with the establishment of the interactions among the polypeptide backbone that would lead to aggregation. In this respect, the tryptophanyl residues located in the A helix of myoglobin seem to play such a crucial role in preventing the main chain from taking over the network of interactions that stabilizes the native three-dimensional structure. The simultaneous replacement of both indole residues determines a deviation from the correct folding pathway leading to protein aggregation and amyloid formation even under physiological conditions (Sirangelo et al. 2002, 2004). Moreover, studies performed with deleted and circularly permuted mutations on sperm whale myoglobin strongly highlight that the native position of the N-terminus is important for the precise structural architecture of the protein (Ribeiro and Ramos 2005). The apo form of the deleted and permuted mutants showed native-like folding and bind heme, but were less stable and exhibited a stronger tendency to aggregate. Moreover, the

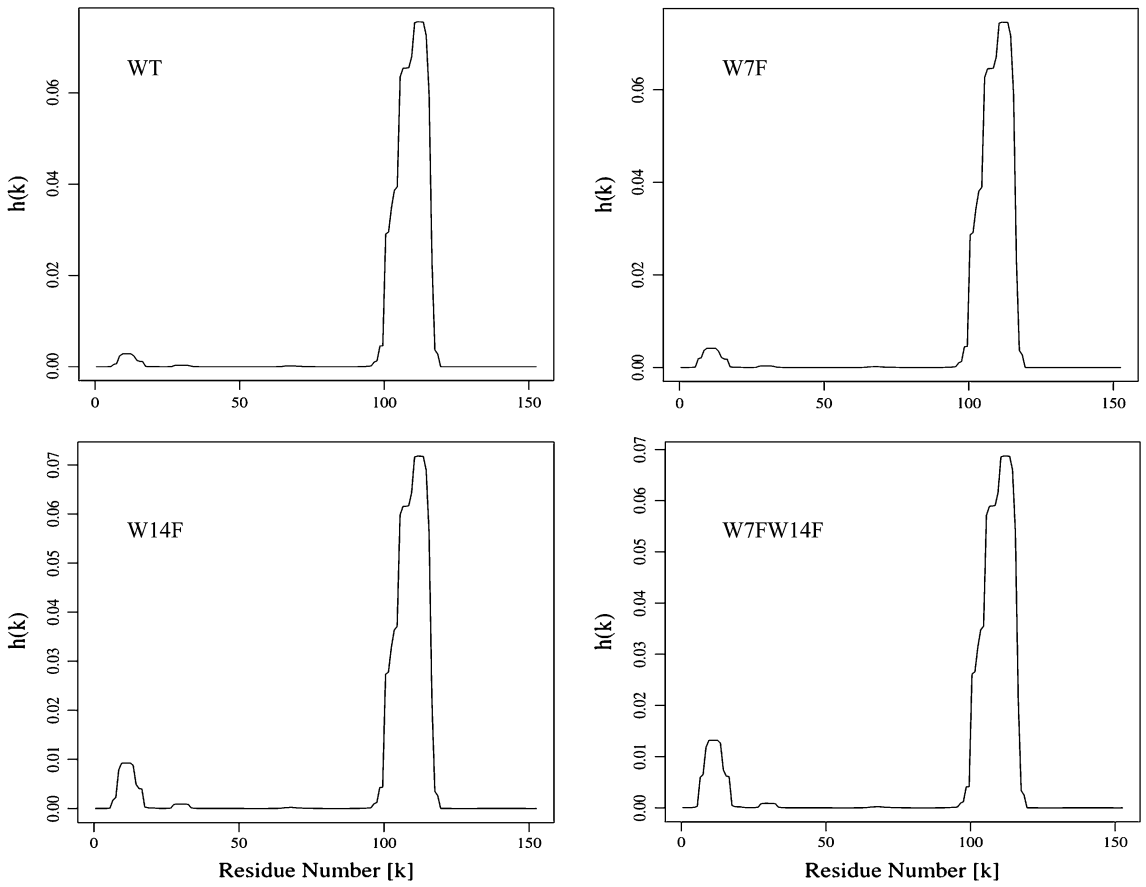

Fig. 9 Prediction of apomyoglobin β-aggregation propensity based on PASTA aggregation scores of wild type and W7F, W14F, and W7FW14F mutants

circularly permuted mutants form cytotoxic fibrils at a rate higher than the wild type (Correa and Ramos 2011).

These considerations prompted us to investigate how the single substitution W → F at either position 7 or 14 affects the protein conformation, dynamics, and stability at both pH 7.0 and 4.0. The latter condition favors the existence of a compact, partially folded intermediate formed by the A, G, and H helices and part of the B helix, with the remainder of the molecule more loosely packed with fluctuating D and E helices (Hughson et al. 1990; Kay and Baldwin 1996; Barrick and Baldwin 1993; Sirangelo et al. 1998, 2003a, b).

Our data show that the apomyoglobin mutant W7F at pH 4.0 contains less α-helical structure and more β-content than wild type, thus indicating that the substitution of the indole residue at position 7 changes the secondary structure organization of the folded portion (AGH subdomain) of the compact intermediate. The CD spectrum of W7F mutant at pH 4.0 is very similar to that of the amyloid-forming mutant and characterized by an increased amount of β-structure. Chow et al. (2003) reported that the 1–36

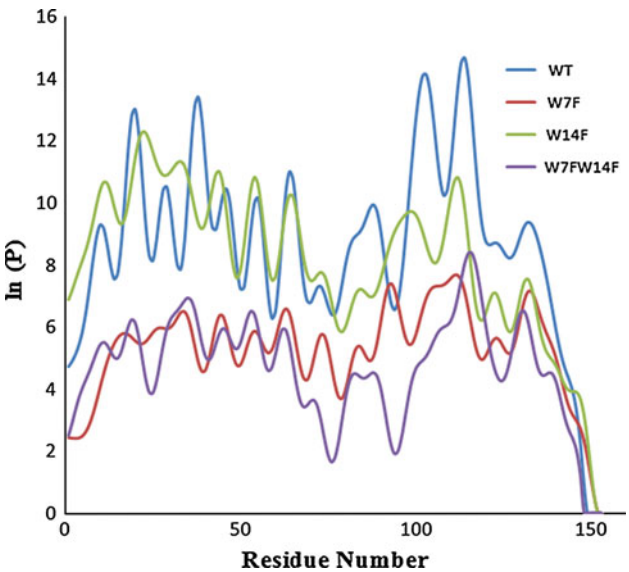

Fig. 10 Camp prediction of wild-type and W7F, W14F, and W7FW14F mutant apomyoglobin. $lnp < 5$ nonprotected residues, $lnp > 5$ protected residues

N-terminal fragment of wild-type apomyoglobin displays a high level of β-structure and forms macroscopic aggregates when the pH gets closer to neutrality.

The limited proteolysis data further corroborate a different organization of the AGH core of the molten globule intermediate of W7F and W7FW14F as compared with wild-type apomyoglobin, as evidenced by the accessibility of G helix to proteolytic cleavage observed for both mutants. The change induced by W7F replacement alters also the interaction between the AGH subdomain and the remainder of the molecule and may, therefore, influence the pattern of side-chain and backbone contacts. Recent studies on permuted mutants (Ribeiro and Ramos 2005) have also indicated that folding of the AGH core helps to constrain the fluctuation of the polypeptide backbone in CDEF subdomain. Moreover, the reciprocal influences of mutations in A helix on E helix and vice versa have been described by Nishimura et al. (2006), who provided strong evidence that docking of the helices A and E is one of the crucial steps of the apomyoglobin folding pathway, with E helix folding and packing occurring when A helix is already folded. This could justify the surprising observation that L69, a side-chain that is known to be located at the interface among helices A, B, E, and G and that mediates packing of the E helix onto the AGH core in the wild-type protein (Nishimura et al. 2006), is protected in the double mutant. Perturbation of the docking of AGH core and E helix has been reported also for other mutations in the A helix (Nishimura et al. 2006), although not as dramatically as in W7FW14F.

Another point of interest is the marked exposition of G helix observed in the equilibrium intermediate formed by W7F and W7FW14F. However, the exposition of the G-helix is not crucial, as indicated by the observation that the single mutant W7F retains a folded structure and does not aggregate. In conclusion, the W $\rightarrow$ F substitution at position 7 changes the secondary (see CD data) and tertiary (see complementary proteolysis) organization of the AGH subdomain. However, this single mutation alone is not able to alter the productive folding pathway of W7F that remains monomeric and soluble at pH 7.0, with an overall three-dimensional (3D) structure very similar to wild type although with a significantly increased accessibility of proteolytic enzymes to H helix. This is further validated by CamP analysis that revealed an increased propensity of this mutant to undergo local unfolding.

The single substitution at position 14 has a less marked effect on the secondary structure of the compact intermediate state populated at pH 4.0. In fact, the CD spectrum of the W14F mutant is the closest one to that of wild-type protein. However, the observed reorganization of the secondary structure (Table 1) induced by W14F substitution determines an increase of the local flexibility documented by fluorescence quenching without affecting the conformational stability of the indole microenvironment.

When the two mutations occur together, their synergic effect determines an uncorrected pairing of the E helix on the preexisting substructure, making the formation of the network of hydrogen bonds of the polypeptide backbone overcome the correct establishment of the tertiary interactions. This conclusion is sustained by the finding that A, B, E, and part of D and G participate in the formation of the amyloid fibril core. This further confirms that the mutations introduced in the N-terminal region are responsible not only for the increased propensity to aggregate but also for perturbing other molecular regions, especially the E and G helices, and involving them in fibril elongation. Prediction analysis evidenced the presence of regions with an intrinsic high β-aggregation propensity that are α-helical structured and buried in the natively folded structure. The simultaneous tryptophanyl replacement not only introduces structural distortion but also increases the overall flexibility of the molecule as indicated by CamP analysis favoring local unfolding and uncorrected pairings. How these uncorrected pairings evolve and intermolecular interactions, leading to fibrils formation, are established has still to be determined.

Another still open question is whether this nonnative docking of the E helix is actually one of the trapped states naturally present on the folding route of apomyoglobin to the native structure. This state, caused by the natural roughness of the protein folding landscape, would become more populated in the simultaneous absence of the two tryptophans. Alternatively, this nonnative docking deviates apomyoglobin from the productive folding pathway to an alternative dead-end route. In both cases, however, the conservation of at least one of the tryptophans in the A helix seems to have been selected by molecular evolutionary pressure to keep myoglobin on the pathway to its native structure.

Acknowledgments This work has been supported by a grant from Regione Campania (DGR 2270, Dec 30, 2006).

References

Aurora R, Creamer TP, Srinivasan R, Rose GD (1997) Local interactions in protein folding: lessons from the alpha-helix. J Biol Chem 272:1413–1416

Baldwin RL (2003) In search of the energetic role of peptide hydrogen bonds. J Biol Chem 278:17581–17588

Baldwin RL, Rose GD (1999) Is protein folding hierarchic? II. Folding intermediates and transition states. Trends Biochem Sci 24:77–83

Barrick D, Baldwin RL (1993) Stein and Moore award address the molten globule state intermediate of apomyoglobin and the process of protein folding. Protein Sci 2:869–876

Ben-Zvi AP, Goloubinoff P (2001) Review: mechanisms of disaggregation and refolding of stable protein aggregates by molecular chaperones. J Struct Biol 135:84–93

Canet D, Last AM, Tito P, Sunde M, Spencer A, Archer DB, Redfield C, Robinson CV, Dobson CM (2002) Local cooperativity in the unfolding of an amyloidogenic variant of human lysozyme. Nat Struct Biol 9:308–315

Chiti F, Calamai M, Taddei N, Stefani M, Ramponi G, Dobson CM (2002) Studies of the aggregation of mutant proteins in vitro provide insights into the genetics of amyloid diseases. Proc Natl Acad Sci USA 99:16419–16426

Chow CC, Chow C, Raghunathan V, Huppert TJ, Kimball EB, Cavagnero S (2003) Chain length dependence of apomyoglobin folding: structural evolution from misfolded sheets to native helices. Biochemistry 42:7090–7099

Ciani B, Hutchinson EG, Sessions RB, Woolfson DN (2002) A designed system for assessing how sequence affects alpha to beta conformational transitions in proteins. J Biol Chem 277:10150–10155

Correa DHA, Ramos CHI (2011) Amyloid fibril formation by circularly permuted and C-terminally deleted mutants. Int J Biol Macromol 48:583–588

Dill KA (1985) Theory for the folding and stability of globular proteins. Biochemistry 24:1501–1509

Dobson CM (1999) Protein misfolding, evolution and disease. Trends Biochem Sci 24:329–332

Dobson CM (2002) Getting out of shape. Nature 418:729–730

Dyuysekina AE, Dolgikh DA, Samatova (Baryshnikova) EN, Tiktopulo EI, Balobanov VA, Bychkova VE (2008) pH-induced equilibrium unfolding of apomyoglobin: substitutions at conserved Trp14 and Met131 and non-conserved Val17 positions. Biochemistry (Moscow) 73:693–701

Edelhoch H (1967) Spectroscopic determination of tryptophan and tyrosine in proteins. Biochemistry 6:1948–1954

Eftink MR, Ghiron CA (1976) Exposure of tryptophanyl residues in proteins. Quantitative determination by fluorescence quenching studies. Biochemistry 15:672–680

Eliezer D, Wright PE (1996) Is apoMb a molten globule? Structural characterization by NMR. J Mol Biol 263:531–538

Eliezer D, Yao Y, Dyson HJ, Wright PE (1998) Structural and dynamic characterization of partially folded states of apomyoglobin and implications of protein folding. Nat Struct Biol 5:148–155

Fandrich M, Forge V, Buder K, Kittler M, Dobson CM, Diekmann S (2003) Myoglobin forms amyloid fibrils by association of unfolded polypeptide segments. Proc Natl Acad Sci USA 100:15463–15468

Fernandez-Escamilla AM, Rousseau F, Schymkowitz J, Serrano L (2004) Prediction of sequence-dependent and mutational effects on the aggregation of peptides and proteins. Nat Biotechnol 22:1302–1306

Fontana A, Zambonin M, Polverino de Laureto P, De Filippis V, Clementi A, Scaramella E (1997) Probing the conformational state of apomyoglobin by limited proteolysis. J Mol Biol 266:223–230

Hughson FM, Wright PE, Baldwin RL (1990) Structural characterization of a partly folded apomyoglobin intermediate. Science 249:1544–1548

Hurle MR, Helms LR, Li L, Chan W, Wetzel R (1994) A role for destabilizing amino acid replacements in light-chain amyloidosis. Proc Natl Acad Sci USA 91:5446–5450

Iannuzzi C, Vilasi S, Portaccio M, Irace G, Sirangelo I (2007) Heme binding inhibits the fibrillization of amyloidogenic apomyoglobin and determines lack of aggregate cytotoxicity. Protein Sci 16:507–516

Irace G, Balestrieri C, Parlato G, Servillo L, Colonna G (1981) Tryptophanyl fluorescence heterogeneity of apomyoglobins. Correlation with the presence of two distinct structural domains. Biochemistry 20:792–799

Jamin M (2005) The folding process of apomyoglobin. Protein Pept Lett 12:229–234

Jennings PA, Wright PE (1993) Formation of a molten globule intermediate early in the kinetic folding pathway of apomyoglobin. Science 262:892–896

Kauzmann W (1959) Some factors in the interpretation of protein denaturation. Adv Protein Chem 14:1–63

Kay MS, Baldwin RL (1996) Packing interactions in the apomyglobin folding intermediate. Nat Struct Biol 3:439–445

Kelly JW (1996) Alternative conformations of amyloidogenic proteins govern their behaviour. Curr Opin Struct Biol 6:11–17

Kim PS, Baldwin RL (1990) Intermediates in the folding reactions of small proteins. Annu Rev Biochem 59:631–660

Kim YJ, Kim YA, Park N, Son HS, Kim KS, Hahn JH (2005) Structural characterization of the molten globule state of apomyoglobin by limited proteolysis and HPLC-mass spectrometry. Biochemistry 44:7490–7496

Konno T (2001) Amyloid-induced aggregation and precipitation of soluble proteins: an electrostatic contribution of the Alzheimer's beta (25–35) amyloid fibril. Biochemistry 40:2148–2154

Kopito RR (2000) Aggresomes, inclusion bodies and protein aggregation. Trends Cell Biol 10:524–530

Laemmli UK (1970) Cleavage of structural proteins during the assembly of head of bacteriophage T4. Nature 227:680–685

Monsellier E, Ramazzotti M, de Laureto PP, Tartaglia GG, Taddei N, Fontana A, Vendruscolo M, Chiti F (2007) The distribution of residues in a polypeptide sequence is a determinant of aggregation optimized by evolution. Biophys J 93(12):4382–4391

Monti M, Amoresano A, Giorgetti S, Bellotti V, Pucci P (2005) Limited proteolysis in the investigation of beta2-microglobulin amyloidogenic and fibrillar states. Biochim Biophys Acta 1753:44–50

Niraula TN, Haraoka K, Ando Y, Li H, Yamada H, Akasaka K (2002) Decreased thermodynamic stability as a crucial factor for familial amyloidotic polyneuropathy. J Mol Biol 320:333–342

Nishimura C, Dyson J, Wright PE (2006) Identification of native and non-native structure in kinetic folding intermediates of apomyoglobin. J Mol Biol 355:139–156

Quintas A, Vaz DC, Cardoso I, Saraiva MJ, Brito RM (2001) Tetramer dissociation and monomer partial unfolding precedes protofibril formation in amyloidogenic transthyretin variants. J Biol Chem 276:27207–27213

Ribeiro EA Jr, Ramos CHI (2005) Circular permutation and deletion of myoglobin indicate that the correct position of its N-terminus is required foe native stability and solubility but not for native-like heme binding and folding. Biochemistry 44:4699–4709

Rochet JC, Lansbury PT Jr (2000) Amyloid fibrillogenesis: themes and variations. Curr Opin Struct Biol 10:60–68

Sirangelo I, Bismuto E, Tavassi S, Irace G (1998) Apomyoglobin folding intermediates characterized by the hydrophobic fluorescent probe 8-anilino-1-naphthalene sulfonate. Biochem Biophys Acta 1385:69–77

Sirangelo I, Tavassi S, Martelli PL, Casadio R, Irace G (2000) The effect of tryptophanyl substitution on folding and structure of myoglobin. Eur J Biochem 267:3937–3945

Sirangelo I, Malmo C, Casillo M, Mezzogiorno A, Papa M, Irace G (2002) Tryptophanyl substitutions in apomyoglobin determine protein aggregation and amyloid-like fibril formation at physiological pH. J Biol Chem 277:45887–45891

Sirangelo I, Dal Piaz F, Malmo C, Casillo M, Birolo L, Pucci P, Marino G, Irace G (2003a) Hexafluoroisopropanol and acid

destabilized forms of apomyoglobin exhibit structural differences. Biochemistry 42:312–319

Sirangelo I, Iannuzzi C, Malmo C, Irace G (2003b) Tryptophanyl substitutions in apomyoglobin affect conformation and dynamic properties of AGH subdomain. Biopolymers 70:649–654

Sirangelo I, Malmo C, Iannuzzi C, Mezzogiorno A, Bianco MR, Papa M, Irace G (2004) Fibrillogenesis and cytotoxic activity of the amyloid-forming apomyoglobin mutant W7FW14F. J Biol Chem 279:13183–13189

Springer BA, Sligar SG (1987) High-level expression of sperm whale myoglobin in *Escherichia coli*. Proc Natl Acad Sci USA 84:8961–8965

Sreerama N, Woody RW (2000) Estimation of protein secondary structure from dichroism circular spectra: comparison of CONTIN, SELCON, and CDSSTR methods with an expanded reference set. Anal Biochem 287:252–260

Tanford C (1973) The hydrophobic effect. Wiley, New York, pp 120–125

Tartaglia GG, Cavalli A, Vendruscolo M (2007) Prediction of local structural stabilities of proteins from their amino acid sequences. Structure 15:139–143

Tartaglia GG, Pawar AP, Campioni S, Dobson CM, Chiti F, Vendruscolo M (2008) Prediction of aggregation-prone regions in structured proteins. J Mol Biol 380:425–436

Teale FWJ (1959) Cleavage of the heme protein by acid methylethylketone. Biochim Biophys Acta 35:543

Tjernberg L, Hosia W, Bark N, Thyberg J, Johansson J (2002) Charge attraction and beta propensity are necessary for amyloid fibril formation from tetrapeptides. J Biol Chem 277:43243–43246

Trovato A, Seno F, Tosatto SCE (2007) The PASTA server for protein aggregation prediction. Protein Eng Des Sel 20(10):521–523

Tsui V, Garcia C, Cavagnero S, Siuzdak G, Dyson HJ, Wright PE (1999) Quench-flow experiments combined with mass spectrometry show apomyoglobin folds through an obligatory intermediate. Protein Sci 8:45–49

Uzawa T, Akiyama S, Kimura T, Takahashi S, Ishimori K, Morishima I, Fujisawa T (2004) Collapse and search dynamics of apomyoglobin folding revealed by submillisecond observations of alpha-helical content and compactness. Proc Natl Acad Sci USA 101:1171–1176

Vilasi S, Sarcina R, Maritato R, De Simone A, Irace G, Sirangelo I (2011) Heparin induces harmless fibril formation in amyloidogenic W7FW14F apomyoglobin and amyloid aggregation in wild-type protein in vitro. PLoS ONE 6(7):e22076

Wetlaufer D (1962) Ultraviolet spectra of proteins and aminoacids. Adv Protein Chem 17(303):390